APPENDIX 1. ANALYTICAL METHODS

A1.1. Whole-rock geochemical analysis

Fresh rock samples were crushed, hand-picked and powdered to a grain size <200 mesh at Yuneng Mineral Separation Service Company at Langfang, Hebei Province, China. Concentrations of major and trace elements of fourteen samples were analyzed at the State Key Laboratory of Geological Processes and Mineral Resources, China University of Geosciences (Wuhan) by the X-ray fluorescence (XFR) on fused glass disks and inductively coupled plasma-mass (ICP-MS) using Agilent 7700e, respectively. The detailed analytical information was described by Yang et al. (2005) and Liu et al. (2008a). Analytical uncertainties for major and trace elements are generally better than 5% and 10%, respectively.

A1.2. Zircon U–Pb dating and trace element analyses

Zircons from five samples were separated by conventional density and magmatic techniques at the laboratory of the Geological Team of Hebei Province, China. Then separated grains were mounted in epoxy resin and polished. Cathodoluminescence (CL) images were taken at the Institute of Geology, Chinese Academy of Geological Sciences (Beijing) to reveal the internal textures and help select suitable spots for zircon in situ analyses.

In situ zircon U–Pb single-spot dating of five samples, synchronously with trace element analyses, were conducted using a beam diameter of 35 μm by laser ablation

inductively coupled plasma mass spectrometry (LA-ICP-MS) using an Agilent 7900 ICP-MS system with New Wave 193UC excimer ArF laser at the Mineral Laser Microprobe Analysis Laboratory (Milma Lab), China University of Geosciences (Beijing) (CUGB). The detailed setting parameters for instruments and experimental process were listed in Zhang et al. (2019). Zircon 91500 and glass NIST SRM 610 were used as external standards for correcting U–Pb dating and trace element calibration, respectively. Zircon GJ-1 (Jackson et al. 2004) and Plešovice (Sláma et al. 2008) were treated as unknown samples and inserted between zircon 91500 and the samples (e.g., 2 zircon 91500 + 1 GJ-1 + 1 Plešovice + 6–8 samples + 2 zircon 91500). A Microsoft Excel-based software ICPMSDataCal (Liu et al. 2008b, 2010) was used to perform off-line data processing and conduction. Procedure ComPbCorr#3.15 (Andersen 2002) was used for common Pb corrections. Isoplot 4.15 (Ludwig 2012) was used to plot concordia diagrams and for $^{206}Pb/^{238}U$ weighted mean calculations.

Zircon LA-ICP-MS U–Pb age and trace element scanning (mapping) from one sample (13MD07-1) were carried out synchronously at the Milma Lab using the same laser and ICP-MS. The laser repletion rate was 8 Hz and the fluence was 5 J/cm^2 for all experiments. NIST SRM 610 glass reference material was used to tune the mass spectrometer to yield stable Th/U ratios and low $^{232}Th^{16}O/^{232}Th$ production rates before geological samples analyses. In order to avoid the contamination of mineral and melt inclusions for trace element analyses, the signals with peaks in data processing were abandoned.

Zircon age and element maps were made by successively acquiring adjacent line

scans to produce a rectangular area on sample. Different laser spot size was used, which depends on mineral size and interest area. To obtain high resolution of zircon, small laser spot size of 7 μm was chose in this experiment. The line scan speed need to integral multiple to the spot size (scan speed = 7 μm/s). Geochemical standard reference samples GSD-1 and GSE-1 were used as the external standards in experiment. Software LAMTrace was used for data processing and mapping of U–Pb age and trace element (Jackson 2008).

A1.3. Zircon Hf–O isotopic analysis

In situ zircon O isotopic analyses of two sample (13MD02-1 and 13MD06-2) were conducted using a Cameca IMS 1280-HR at the SIMS Laboratory of Guangzhou Institute of Geochemistry, Chinese Academy of Sciences. The zircon Penglai is used as an external reference material to calibrate the instrumental mass fractionation. The zircon Qinghu is used as the unknown samples that was inserted between Penglai and the samples, which yield 5.49 ± 0.14‰ (2SD) (n=7), consistent with the recommended values within error (2SD). The analytical beam diameter is 10×20 μm. More detailed analytical and data processing information was reported by Yang et al. (2018).

Following O isotopic analyses, zircon Hf isotopes were conducted on or nearby the same location overlapped Hf spots. It was performed by a Neptune Plus multi collector (MC)-ICP-MS coupled to a New Wave 193 excimer ArF laser ablation system at the Milma Lab, CUGB, with a beam diameter of 35 μm, laser pulse frequency of 8 Hz and energy density of 3.7 J/cm^2. Makeup gas of argon and carrier gas of helium with

the addition of nitrogen mixed in a T–branch pipe prior to introduction into the MC-ICP-MS.

In the experiment, L4 to H3 Faraday cups were used to collect ^{171}Yb, ^{173}Yb, ^{175}Lu, ^{176}Hf, ^{177}Hf, ^{178}Hf, ^{179}Hf, and ^{180}Hf, respectively with the integration time of 0.131 s. The carrier and makeup gas flows were optimized by a line scan (spot size of 35 μm and scan speed of 5 μm/s) ablating NIST SRM 610 to obtain maximum signal intensity for ^{232}Th, while minimizing ^{232}Th^{16}O/^{232}Th ratio. For each analysis, 50 s integration for gas blank and 50 s integration for signal collection were set up with a total of 800 cycles of raw data. Zircon 91500 (Blichert–Toft 2008) was used as an external standard for correcting mass discrimination. Zircon Plešovice (Sláma et al. 2008) was treated as unknown sample that was inserted between zircon 91500 and the samples (e.g., 2 zircon 91500 + 1 Plešovice + 6–10 samples + 2 zircon 91500). Raw data was converted by Neptune Plus software and performed using Iolite software (Paton et al. 2011). The obtained ^{176}Hf/^{177}Hf ratio of Plešovice was 0.282490 ± 18 (2SD) (n=6), consistent with the recommended values within error (2SD).

The initial ^{176}Hf/^{177}Hf ratios and εHf(t) values were calculated with the reference to the chondritic reservoir (CHUR) at the time of zircon growth from the magmas. The decay constant for ^{176}Lu of 1.867×10^{-11} year $^{-1}$ (Söderlund et al. 2004), the chondritic ^{176}Hf/^{177}Hf ratio of 0.282785 and ^{176}Lu/^{177}Hf ratio of 0.0336 (Bouvier et al. 2008) were adopted. Depleted mantle model ages (T_{DM}) were calculated with reference to the depleted mantle at a present–day ^{176}Hf/^{177}Hf ratio of 0.28325, and ^{176}Lu/^{177}Hf = 0.0384 (Griffin et al. 2000). The Hf isotope crustal model age (T_{DM}^{C}) was calculated by assuming

that its parental magma was derived from an average continental crust, with $^{176}Lu/^{177}Hf$ = 0.015, that originated from the depleted mantle source (Griffin et al. 2002).

A1.4. Quartz Ti analyses

CL images of quartz phenocrysts randomly selected in thin sections from four rhyolite samples (13MD02-4, 13MD05-1, 13MD06-2, 13MD07-1) were obtained at Beijing Createch Testing Technology Co. Ltd. Trace elements, especially Ti content in quartz were investigated at Milma Lab, CUGB by LA-ICP-MS. In the experiments, both 50 μm (Fig. 1) and 75 μm (Fig. 2) beam diameter were chose. The corresponding laser repletion rates were 10 Hz and 8 Hz, respectively. The corresponding fluence were 10 J/cm^2 and 8 J/cm^2, respectively. Glass NIST SRM 610 and 612 were analyzed as external standards, BHVO-2 and BCR-2G were treated as unknown samples that were inserted between external standards and samples. Analytical uncertainty is normally less than 15 %. Raw data was performed using GLITTER software and the SiO_2 content of samples were preset as 99.0 wt %. The Ti-in-Quartz temperature was calculated following the TitaniQ equation described by Wark and Watson (2006). These calculations assume that no significant change in the activity of Ti in the magma during quartz crystallized.

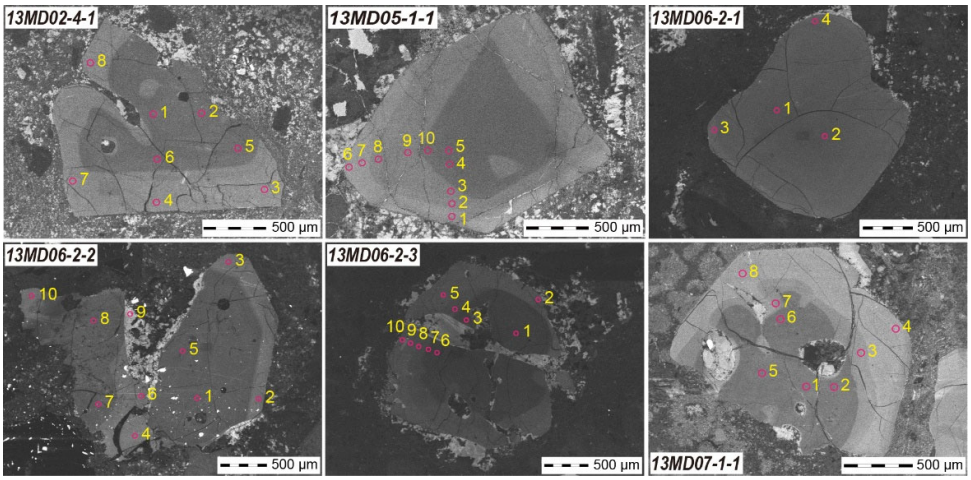

Fig. 1. CL images of quartz phenocrysts selected randomly from four Nuocang HSR samples. The pink circles and yellow numbers denote LA-ICP-MS trace element analyses spots which sizes are 50 μm.

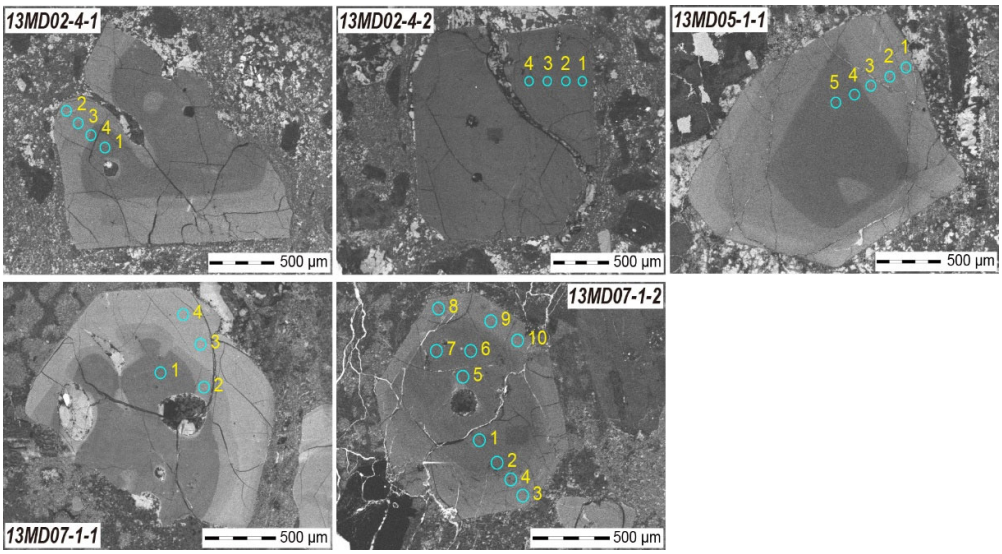

Fig. 2. CL images of quartz phenocrysts selected randomly from three Nuocang HSR samples. The blue circles and yellow numbers denote LA-ICP-MS trace element analyses spots which sizes are 75 μm.

REFERENCES CITED

Andersen, T. (2002) Correction of common lead in U–Pb analyses that do not report ^{204}Pb. Chemical Geology, 192, 59–79.

Blichert-Toft, J. (2008) The Hf isotopic composition of zircon reference material 91500. Chemical Geology, 253, 252–257.

Bouvier, A., Vervoort, J.D., and Patchett, P.J. (2008) The Lu–Hf and Sm–Nd isotopic composition of CHUR: Constraints from unequilibrated chondrites and implications for the bulk composition of terrestrial planets. Earth and Planetary Science Letters, 273, 48–57.

Griffin, W.L., Pearson, N.J., Belousova, E., Jackson, S.E., van Achterbergh, E., O'Reilly, S.Y., and Shee, S.R. (2000) The Hf isotope composition of cratonic mantle: LAM-MC-ICPMS analysis of zircon megacrysts in kimberlites. Geochimica et Cosmochimica Acta, 64, 133–147.

Griffin, W.L., Wang, X., Jackson, S.E, Pearson, N.J., O'Reilly, S.Y., Xu, X.S., and Zhou, X.M. (2002) Zircon chemistry and magma mixing, SE China: In situ analysis of Hf isotopes, Tonglu and Pingtan igneous complexes. Lithos, 61, 237–269.

Jackson, S.E., Pearson, N.J., Griffin, W.L., and Belousova, E.A. (2004) The application of laser ablation-inductively coupled plasma-mass spectrometry to in situ U–Pb zircon geochronology. Chemical Geology, 211, 47–69.

Jackson, S. (2008) LAMTRACE Data Reduction Software for LA-ICP-MS. In P. Sylvester, Ed., Laser Ablation ICP-MS in The Earth Sciences: Current Practices and Outstanding Issues, p. 305–307. Mineralogical Association of Canada.

Liu, Y.S., Zong, K.Q., Kelemen, P.B., and Gao, S. (2008a) Geochemistry and magmatic history of eclogites and ultramafic rocks from the Chinese continental scientific drill hole: Subduction and ultrahigh-pressure metamorphism of lower crustal cumulates. Chemical Geology, 247, 133–153.

Liu, Y.S., Hu, Z.C., Gao, S., Günther, D., Xu, J., Gao, C.G., and Chen, H.H. (2008b) In situ analysis of major and trace elements of anhydrous minerals by LA-ICP-MS without applying an internal standard. Chemical Geology, 257, 34–43.

Liu, Y.S., Hu, Z.C., Zong, K.Q., Gao, C.G., Gao, S., Xu, J., and Chen, H.H. (2010) Reappraisement and refinement of zircon U-Pb isotope and trace element analyses by LA-ICP-MS. Chinese Science Bulletin, 55, 1535–1546.

Ludwig, K. R. (2012) User's Manual for Isoplot 3.75, a Geochronological Toolkit for Microsoft Excel. Berkeley Geochronology Center Special Publication, Berkeley, California, no. 5 (75 pp.)

Paton, C., Hellstrom, J., Paul, B., Woodhead, J., and Hergt, J. (2011) Iolite: Freeware for the visualisation and processing of mass spectrometric data. Journal of Analytical Atomic Spectrometry, 26, 2508–2518.

Sláma, J., Košler, J., Condon, D.J., Crowley, J.L., Gerdes, A., Hanchar, J.M. Matthew, S.A.H, Morris, G.A., Nasdala, L., Norberg, N., Schaltegger, U., Schoene, B, Tubrett, M.N., and Whitehouse, M.J. (2008) Plešovice zircon — A new natural reference material for U–Pb and Hf isotopic microanalysis. Chemical Geology, 249, 1–35.

Söderlund, U., Patchett, P.J., Vervoort, J.D., and Isachsen, C.E. (2004) The ^{176}Lu decay

constant determined by Lu–Hf and U–Pb isotope systematics of Precambrian mafic intrusions. Earth and Planetary Science Letters, 219, 311–324.

Wark, D.A., and Watson, E.B. (2006) TitaniQ: a titanium-in-quartz geothermometer. Contributions to Mineralogy and Petrology, 152, 743–754.

Yang, J.H., Chung, S.L., Wilde, S.A., Wu, F.Y., Chu, M.F., Lo, C.H., and Fan, H.R. (2005) Petrogenesis of post-orogenic syenites in the Sulu Orogenic Belt, East China: geochronological, geochemical and Nd–Sr isotopic evidence. Chemical Geology, 214, 99–125.

Yang, Q., Xia, X.P., Zhang, W.F., Zhang, Y.Q., Xiong, B.Q., Xu, Y.G., Wang, Q., and Wei, G.J. (2018) An evaluation of precision and accuracy of SIMS oxygen isotope analysis. Solid Earth Sciences, 3, 81–86.

Zhang, L.L., Zhu, D.C., Wang, Q., Zhao, Z.D., Liu, D., and Xie, J.C. (2019) Late Cretaceous volcanic rocks in the Sangri area, southern Lhasa Terrane, Tibet: Evidence for oceanic ridge subduction. Lithos, 326–327, 144–157.